

# Development of a Relative Motion Model for Satellite Formation Flying around L2

Jennifer Roberts  
Space Research Centre, School of Engineering,  
Cranfield University, UK

## Abstract

A technique for satellite formation flying modelling in LEO is applied at L2. Analytical solutions to the equations of motion of a hub satellite relative to L2 are used to define a halo reference orbit. An expression for the gravity gradient is obtained at the hub and the linearised equations of motion of the mirror satellites relative to the hub are derived. The relative motion model is implemented in Matlab/Simulink and evaluated for different initial conditions. The analytical solutions to the equations of relative motion are derived. These and other equations of motion are compared to the Satellite Tool Kit numerical orbit propagator.

## Introduction

The autonomous formation flying of multiple spacecraft to replace a single large satellite will be an enabling technology for a number of future missions. A significant space science application is deep space interferometry which requires a number of telescopes to both manoeuvre and maintain formation with unprecedented accuracy. The focus of this study is the ESA mission, Darwin, which has two main objectives: ‘the detection and characterisation of Earth-like planets orbiting other stars and the imaging of astrophysical objects with unprecedented spatial resolution’ [1]. The formation of six telescopes and one hub must be able to operate on a baseline of 50 to 500 metres in a circular planar formation, and achieve a  $1\mu\text{m}$  inter-satellite separation accuracy.

A number of formation flying models have been developed to describe the relative motion between two or more satellites in Low Earth Orbit (LEO). The most fundamental of these are the Hill [6] or Clohessy-Wiltshire equations written in terms of a Cartesian or curvilinear coordinate frame tracing a circular reference orbit around the Earth, and models using Orbit Element Differences to describe relative orbits [10]. Schweighart and Sedwick [12] extended the Hill equations to include the effect of the  $J_2$  perturbation using a force gradient approach. This was extended to time-varying form, verified and applied to linear quadratic regulator (LQR) design and evaluation for the station-keeping task by Roberts and Roberts [9]. In this study the force gradient modelling approach is investigated for satellites formation flying around the L2 Lagrange point using periodic halo motion as a reference.

Significant research has been performed into satellite formation flying for Lagrange point missions. Gurfil and Kasdin [4] also generate a model of relative spacecraft

dynamics by linearising relative to an arbitrary reference trajectory in the circular restricted three-body problem (CR3BP). Linear time-varying differential equations result and a time-varying continuous LQ control law is also developed (using the differential Riccati equation), with disturbance rejection properties. However, their work examines formation flying in the vicinity of Earth in an out-of-the-ecliptic trajectory, and not L2. Their equations are quadratic in terms of distance from the Earth, and the model is not verified. Scheeres and Vinh [11] examine the linearised dynamics for relative motion in an unstable halo orbit in the Hill problem (a simplification of the three-body problem). The time-varying dynamics are approximated over short time intervals and stabilising control laws designed.

In a later paper by Gurfil, Idan and Kasdin [3] the nonlinear equations of relative motion are derived in the context of the elliptical restricted three-body problem (ER3BP). A relative position controller is designed using approximate feedback linearisation via dynamic model inversion, LQR controller design, and neural network design to compensate for the inversion error. In their view, the linearised model is insufficiently accurate to yield the required formation-keeping precision, although sub-5mm precision was obtained in the CR3BP case. However, earlier LEO work [9] demonstrated that the achievement of dynamics modelling improvements for LQR controller design may not be very significant, and the extent to which the linearised models for formation control in Lagrange point orbits are of use is therefore currently being investigated.

Hamilton, Carpenter and Folta [5] apply the LQR control technique with Kalman filtering to formation station-keeping and manoeuvring control in the vicinity of L2 in the CR3BP. The dynamics models used are obtained from software, developed at Purdue University, which calculates accurate Lissajous reference orbits, including the effects of a separate moon, solar radiation pressure, Earth orbit eccentricity and the presence of other planets. A linearised dynamics matrix is also calculated by the software at each epoch for LQR design. The hub is found to track the reference orbit satisfactorily but the drones (or ‘telescopes’) only achieve a tracking accuracy of a few metres when process and measurement noise are included in their simulation. Station-keeping and formation slewing are simulated and fuel costs measured. Howell and Marchand [7] also evaluate the time-varying linearised system matrix along a numerically generated reference orbit in the CR3BP for controller design. Vadali, Bae and Alfriend [14] use the analytical solutions for a periodic orbit in the CR3BP developed by Richardson [8] for formation design. They also apply input feedback linearisation control for formation maintenance, slewing and fuel-balanced reconfiguration.

Segerman and Zedd [13] have recently derived high order solutions to the equations of relative motion for two satellites orbiting L2. The nonlinear equations of motion for the hub (leader) satellite and the telescope satellite are derived separately in the CR3BP, assuming that both are ‘in the vicinity’ of L2. The hub equation is subtracted from the telescope equation and the equation of motion for the telescope relative to the hub results. A series expansion is performed and the terms are evaluated and ordered by magnitude. The frequency of out of plane motion is

adjusted to have the same fundamental period as the in-plane motion to create a planar formation. The analytical solutions to the equations of motion are derived using a Lindstedt-Poincare-type method and compared to numerically integrated solutions. Due to the divergent nature of the relative motion, comparisons were only made over 20 day periods using initial conditions derived from the analytical solutions at time  $t=0$ . It was found for one test case that their solutions approximated well the numerical integration of the two separate CR3BP equations of motion (one for each satellite) for around 5 days in all directions.

In this study, the linearised system dynamics are evaluated at each point on a reference orbit described by the Richardson third-order analytical solution for a periodic halo orbit around L2. This continues previous LEO formation flying work where the relative motion was governed by force gradients. The analytical approach also enables expressions for initial formation conditions, to which relative motion is so sensitive, to be derived. Segerman and Zedd [13] evaluate the modelling error with one example of model verification, and the other references discussed above do not evaluate or specify clearly the modelling error associated with linearisation. In order to design controllers using this formation flying tool, it is necessary to firstly evaluate the modelling error against a suitable numerical orbit propagator. In future, the controllers designed will be flown in the Satellite Tool Kit (STK) Astrogator software, and this was therefore used for model comparison. The gravity gradient model solution in terms of linear distance from L2 (quadratic was also implemented) is compared to similar scenarios in STK, and also the solution of Segerman and Zedd.

## Model development

The standard nonlinear equations of motion with respect to the L2 point for a single satellite flying in the vicinity of L2, in the inertial Cartesian coordinate frame, in the circular restricted three-body problem, are given by equations 1 to 3.

$$\delta \ddot{x} = -\left(\frac{\mu_s \delta x}{\rho_s^3} + \frac{\mu_e \delta x}{\rho_e^3}\right) - \left(\frac{\mu_s (x_o - x_s)}{\rho_s^3} + \frac{\mu_e (x_o - x_e)}{\rho_e^3}\right) + n^2 x_o \quad (1)$$

$$\delta \ddot{y} = -\left(\frac{\mu_s \delta y}{\rho_s^3} + \frac{\mu_e \delta y}{\rho_e^3}\right) \quad (2)$$

$$\delta \ddot{z} = -\left(\frac{\mu_s \delta z}{\rho_s^3} + \frac{\mu_e \delta z}{\rho_e^3}\right) \quad (3)$$

where  $n$  is the mean motion of the Earth-Moon barycentre about the Sun in an assumed circular orbit rotating about the Sun-Earth/Moon barycentre. All terms are illustrated in Figure 1, where ‘Earth’ represents the combined Earth-Moon system.

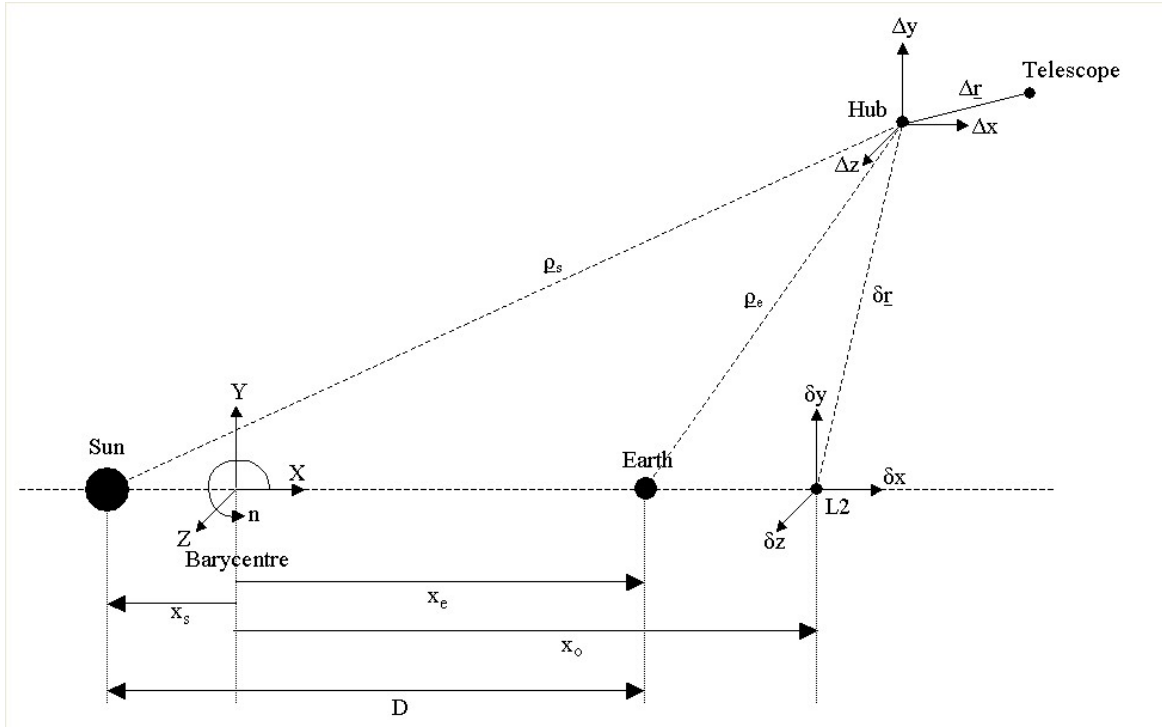


Figure 1: Formation flying parameters in the three-body system

Equations 1 to 3 can be summarised in vector form by equation 4, which describes the motion of satellite number  $N$ . In this case we consider just two satellites, the hub ( $N=1$ ) and a single telescope ( $N=2$ ).

$$\delta \ddot{\underline{r}}_N = \underline{f}_N \quad (4)$$

For relative motion, the nonlinear equations of motion for each satellite must be subtracted, however, the relative motion can be written in linearised form by evaluating the gravity gradient at the hub and multiplying by the distance between the hub and telescope (equation 5).

$$\Delta \ddot{\underline{r}} = \delta \ddot{\underline{r}}_2 - \delta \ddot{\underline{r}}_1 = \underline{f}_2 - \underline{f}_1 = \nabla \underline{f}_1 \cdot \Delta \underline{r} \quad (5)$$

The gravity gradient was evaluated in 3-dimensions for the general case (anywhere in the CR3BP). The equations of relative motion in non-dimensional form, linearised with respect to distance from L2, and for two satellites orbiting specifically the L2 point in the now rotating coordinate system are given by equations 6 to 8 where  $R_s = x_o - x_s$ ,  $R_e = x_o - x_e$ ,  $\rho_m \equiv -x_s$ , and  $(1 - \rho_m) \equiv x_e$ . Distances are in units of Sun-Earth separation ( $D$ ), time is non-dimensionalised with respect to the mean motion,  $n$ , and  $\rho_m$  is also given as the mass ratio  $M_{\text{Earth/Moon}} / (M_{\text{Earth/Moon}} + M_{\text{Sun}})$ . All other terms are defined in Figure 1.

$$\begin{aligned} \Delta\ddot{x} - 2\Delta\dot{y} - \Delta x = & \left[ -(1 - \rho_m) \left( \frac{1}{R_s^3} - \frac{3}{R_s^5} (x_o + \rho_m) \{2\delta x + x_o + \rho_m\} \right) \dots \right. \\ & \left. \dots - \rho_m \left( \frac{1}{R_e^3} - \frac{3}{R_e^5} (x_o - 1 + \rho_m) \{2\delta x + x_o - 1 + \rho_m\} \right) \right] \Delta x \end{aligned} \quad (6)$$

$$\begin{aligned} \Delta\ddot{y} + 2\Delta\dot{x} - \Delta y = & \left[ 3\delta y \left( \frac{(1 - \rho_m)(x_o + \rho_m)}{R_s^5} + \frac{\rho_m(x_o - 1 + \rho_m)}{R_e^5} \right) \right] \Delta x \dots \\ \dots + & \left[ -(1 - \rho_m) \left( \frac{1}{R_s^3} - \frac{3(x_o + \rho_m)\delta x}{R_s^5} \right) - \rho_m \left( \frac{1}{R_e^3} - \frac{3(x_o - 1 + \rho_m)\delta x}{R_e^5} \right) \right] \Delta y \end{aligned} \quad (7)$$

$$\begin{aligned} \Delta\ddot{z} = & \left[ 3\delta z \left( \frac{(1 - \rho_m)(x_o + \rho_m)}{R_s^5} + \frac{\rho_m(x_o - 1 + \rho_m)}{R_e^5} \right) \right] \Delta x \dots \\ \dots + & \left[ -(1 - \rho_m) \left( \frac{1}{R_s^3} - \frac{3(x_o + \rho_m)\delta x}{R_s^5} \right) - \rho_m \left( \frac{1}{R_e^3} - \frac{3(x_o - 1 + \rho_m)\delta x}{R_e^5} \right) \right] \Delta z \end{aligned} \quad (8)$$

The gravity gradient must be evaluated at the hub telescope, and therefore its location must be known. In these equations, this is achieved through providing values for the  $\delta x, \delta y, \delta z$  terms, which are the separation of the hub satellite from the L2 point. This also provides the user with the opportunity to prescribe the orbit of the hub telescope (eliminating the divergent modes of halo motion) in order to focus on the control of relative satellite motion.

The hub orbit was selected to be a periodic halo orbit, although a Lissajous could also be prescribed. The third-order analytical solution to the full three-dimensional equations of motion for periodic motion about L2 in the CR3BP developed by Richardson [8] was applied. The hub motion is given by equations 9, 10 and 11 where  $A_x, A_y,$  and  $A_z$  in the x, y, z directions respectively are the amplitudes of the linearised halo solution,  $\tau_1$  is the independent variable relating frequency correction and orbital rate to time and the remaining terms are constants associated with the Linsdtedt-Poincare type method of solution used. An amplitude constraint relationship was derived and the satellites can be initialised at any point on the halo.

$$\delta x = a_{21}A_x^2 + a_{22}A_z^2 - A_x \cos \tau_1 + (a_{23}A_x^2 - a_{24}A_z^2) \cos 2\tau_1 + (a_{31}A_x^3 - a_{32}A_xA_z^2) \cos 3\tau_1 \quad (9)$$

$$\delta y = kA_x \sin \tau_1 + (b_{21}A_x^2 - b_{22}A_z^2) \sin 2\tau_1 + (b_{31}A_x^3 - b_{32}A_xA_z^2) \sin 3\tau_1 \quad (10)$$

$$\delta z = \delta_n A_z \cos \tau_1 + \delta_n d_{21} A_x A_z (\cos 2\tau_1 - 3) + \delta_n (d_{32} A_z A_x^2 - d_{31} A_z^3) \cos 3\tau_1 \quad (11)$$

## Solutions and initial conditions

### Hub satellite

For the model verification, the two satellites in the formation are propagated separately in STK. The initial position of the hub (or leader) relative to L2 is found by setting time  $t=0$  (equivalent to  $\tau_1 = 0$ ) in equations 9, 10 and 11.  $\delta y_o$  becomes zero, but  $\delta x_o$  and  $\delta z_o$  are non-zero functions of the constants and linear solution halo amplitudes  $A_x$  and  $A_z$ . The initial velocity conditions,  $\delta \dot{x}_o, \delta \dot{y}_o, \delta \dot{z}_o$  can be found by differentiating equations 9, 10 and 11, and setting time  $t=0$ . These values were compared to the initial conditions approximated by the linear solution conditions for removal of divergent modes (equations 12 and 13) where  $\lambda$  is the frequency of the in-plane oscillatory mode and  $k$  arises from the elimination of exponential terms in the linearised solutions.

$$\delta \dot{x}_o = \frac{\lambda}{k} \delta y_o \quad (12)$$

$$\delta \dot{y}_o = -k\lambda \delta x_o \quad (13)$$

### Telescope satellite

The solutions to equations 6, 7 and 8 describing the telescope with respect to the hub on a halo orbit were derived using a state transition matrix approach with the time-varying state matrix. By substituting for  $\delta x, \delta y, \delta z$  into equations 6, 7 and 8, and integrating, solutions were generated in the form of equation 14.

$$\Delta \underline{r}(t) = e^{\int A(t) dt} \Delta \underline{r}(0) \quad (14)$$

By applying the exponential expansion

$$e^{At} = I + At... \quad (15)$$

a solution for relative motion was obtained and a relationship between the initial conditions ( $\Delta \underline{r}(0)$ ) was found to eliminate secular terms. For the in-plane (x-y) motion, these are given by equations (16) and (17).

$$\Delta \dot{y}_o = -\left[ \frac{1}{2} - \frac{(1-\rho_m)}{2} \left[ \frac{1}{R_s^3} - \frac{3(x_o + \rho_m)^2}{R_s^5} \right] - \frac{\rho_m}{2} \left[ \frac{1}{R_e^3} - \frac{3(x_o - 1 + \rho_m)^2}{R_e^5} \right] + \left( \frac{3(1-\rho_m)(x_o + \rho_m)}{R_s^5} + \frac{3\rho_m(x_o - 1 + \rho_m)}{R_e^5} \right) (a_{21}A_x^2 + a_{22}A_z^2) \right] \Delta x_o \quad (16)$$

$$\Delta \dot{x}_o = \frac{1}{2} \left[ 1 - \frac{(1-\rho_m)}{R_s^3} - \frac{\rho_m}{R_e^3} + \left( \frac{3(1-\rho_m)(x_o + \rho_m)}{R_s^5} + \frac{3\rho_m(x_o - 1 + \rho_m)}{R_e^5} \right) (a_{21}A_x^2 + a_{22}A_z^2) \right] \Delta y_o \quad (17)$$

The analytical solutions derived by Segerman and Zedd [13] were also implemented and evaluated at time  $t=0$  for comparison of initial conditions.

### ***Initial conditions comparison***

For the test case described in [13], the initial position and velocity of the hub satellite with respect to L2 and the relative initial conditions with respect to the hub satellite, obtained using the different methods described above, are summarised in Table 1. The initial y-velocity given by the derivative of equation 10 (Richardson) is approximated by the y-velocity predicted by equation 13. Of interest in the relative motion initial separations and velocities is again the y-velocity. The application of the higher order relative motion model of Segerman and Zedd (SZ) gave a slightly lower initial y-velocity than that predicted by linearised gravity gradient model (equation 16) of approximately 4.4m/day.

<b>HUB Initial Conditions</b>		<b>TELESCOPE-HUB Relative Initial Conditions</b>	
Linear Amplitude Ax (km)	227219.42	Position $\Delta x_o$ (m)	-64.7796
Linear Amplitude Ay (km)	724200.94	Position $\Delta y_o$ (m)	0
Linear Amplitude Az (km)	250000.00	Position $\Delta z_o$ (m)	26.7391
Velocity $\dot{x}_{o1}$ (km/s)	0	Velocity (SZ model) $\Delta \dot{x}_o$ (m/day)	0
Velocity (Richardson) $\dot{y}_{o1}$ (km/s)	0.3134925	Velocity (SZ model) $\Delta \dot{y}_o$ (m/day)	4.4205
Velocity $\dot{z}_{o1}$ (km/s)	0	Velocity (SZ model) $\Delta \dot{z}_o$ (m/day)	0
Velocity (Linear Approx.) $\dot{y}_{o1}$ (km/s)	0.3631100	Velocity (Gravity gradient model) $\Delta \dot{x}_o$ (m/day)	0
		Velocity (Gravity gradient model) $\Delta \dot{y}_o$ (m/day)	4.9011

Table 1: Hub and telescope initial conditions

### **Model and STK scenario implementation**

The formation flying models were implemented in a Matlab/Simulink environment for comparison with similar STK scenarios. All equations were non-dimensionalised and the analytically derived initial conditions for all models were compared for different test cases.

The ‘real’ satellite behaviour was propagated using STK Astrogator, a high precision orbit propagator, incorporating solar, terrestrial and lunar effects. A Cartesian axis system was created at the L2 point, and initial conditions were provided to each satellite as Cartesian position and velocity relative to L2. The hub was given the prescribed halo initial conditions, and the telescope was provided with initial conditions given in form by equation 18 where  $X_0$  is the vector of initial positions and velocities.

$$\delta X_0^{Telescope} = \delta X_0^{Hub} + \Delta X_0^{Relative} \quad (18)$$

Absolute motion of each satellite was extracted through the STK reporting tool and differenced to obtain relative motion of the telescope with respect to the hub.

Unlike the equations of motion in the CR3BP, the eccentricity of the Earth’s orbit significantly affects the location of the L2 point. STK propagations were run at two different epochs, six months apart, but this did not appear to affect the relative motion dynamics significantly. The propagation time step was fixed at 1 hour for both the Matlab models and STK during the 180-day scenario (duration of the analytically derived halo orbit period). Subsequent analyses focussed on the first 20 days of orbit, as without control, the numerical solution would diverge from the ‘ideal’ halo orbit.

### Model comparison

One example of gravity gradient model comparison with STK is included in this paper. A Darwin-type orbit was selected, based on the ESA Darwin Concept and Feasibility Study [1] and the relationship between insertion delta-V and amplitude of a halo orbit derived by Farquhar [2]. The following initial conditions (Table 2) were applied to the formation. Note that for zero delta-V insertion into a halo orbit  $A_y$  was 780000km (and therefore  $A_x$  was 244726.7km, and  $A_z$  was 368380.8km). For these linear amplitudes of motion, the hub satellite initial position was out-of-the-ecliptic by  $z_{01}$ km, and on the Earth side of L2 on the Sun-Earth line. The telescope was selected to be separated by from the hub by 100 metres ( $\Delta x_o$ ), parallel to the Sun-Earth line, and to remain in the hub plane. The gravity gradient model for the reduction of secular motion suggests an initial relative y-velocity of 7.5659m/day, which is equivalent to the very small value of 87.6 $\mu$ m/sec.

HUB Initial Conditions		TELESCOPE-HUB Relative Initial Conditions	
Initial Position $x_{01}$ (km)	-319112	Position $\Delta x_o$ (m)	-100
Initial Position $y_{01}$ (km)	0	Position $\Delta y_o$ (m)	0
Initial Position $z_{01}$ (km)	329681	Position $\Delta z_o$ (m)	0
Velocity $\dot{x}_{01}, \dot{z}_{01}$ (km/s)	0	Velocity (Gravity gradient model) $\Delta \dot{x}_o$ (m/day)	0
Velocity (Richardson) $\dot{y}_{01}$ (km/s)	0.3422590	Velocity (Gravity gradient model) $\Delta \dot{y}_o$ (m/day)	7.5659

Table 2: DARWIN hub and telescope initial conditions

### Halo motion

The third-order analytical solution for the prescribed halo orbit [8] was compared to the motion of the hub satellite in STK. Figure 2 illustrates the analytical halo motion and the difference between this and the hub motion propagated in STK over a period of 20 days. The hub motion in STK does appear to perform a partial halo before diverging onto an alternative trajectory.



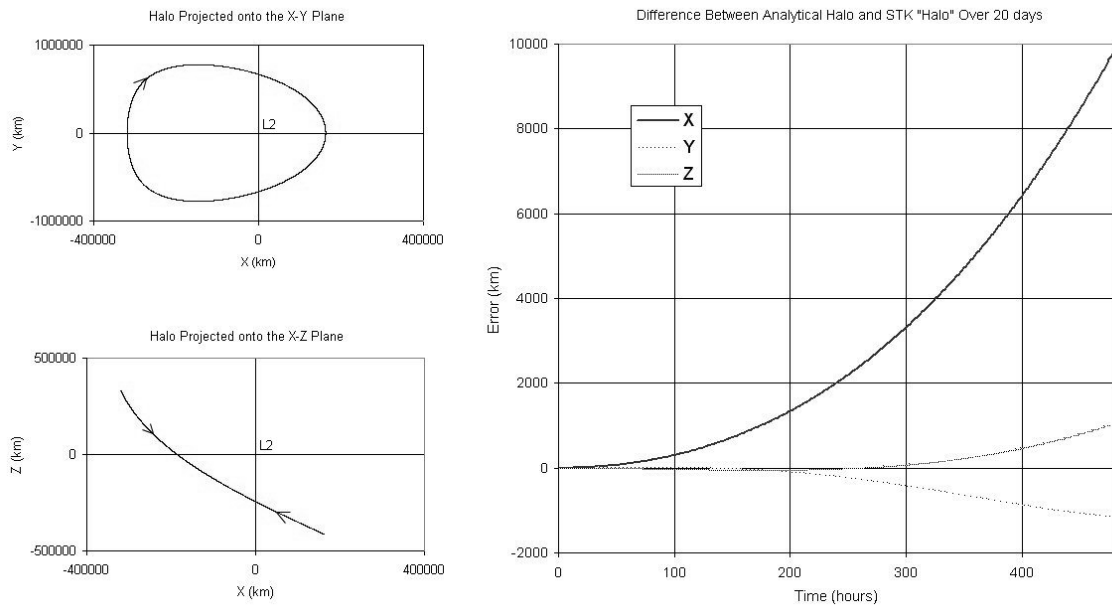


Figure 2: DARWIN-type halo orbit, and halo modelling error

After 20 days, the uncontrolled STK ‘halo’ has diverged from the analytical halo motion by 9854km in X, 1044km in Y, and 1150km in Z for a halo orbit of approximately 780000km in Y-dimension. The divergence is significantly less over shorter periods of time, and if we assume frequent control of the hub satellite (for example, every quarter of a halo orbit), the analytical halo is sufficiently accurate to represent the hub motion. This was confirmed by evaluating the gravity gradient model along both the analytical and STK reference orbits and examining their effects on relative motion over a few days. A few kilometres in hub halo error did not significantly affect the relative motion predicted by the gravity gradient model.

### ***Relative motion***

The relative motion in the x, y and z directions, predicted by both STK and the gravity gradient model are illustrated in Figure 3. In the x direction, STK predicts that the satellites will separate by a further 14.2m in 20 days. However, the gravity gradient model indicates that the satellites will in fact be moving closer together (by 18.5m). The error in predicted motion is very small at 1.6m/day and upon examination of the x-equation of motion (equation 6), it was found that the cause of the change in the x direction was due to the y-velocity contribution. The equation was extremely sensitive to the relative y-velocity, which at  $87.6\mu\text{m/s}$  is very small and difficult to control. This initial condition was evaluated using an approximate model, and a very small error in the approximation would make a very large difference to the relative motion obtained.

In the CR3BP, the physical location of the satellites can be visualised. The telescope is nearer to the Earth than the hub, while the hub is closer to L2. The hub is given an initial y-velocity ( $\dot{y}_{01}$  in Table 2) and increases in altitude, pulling away from the Earth. The hub then experiences a growing centrifugal force, which in

combination with the Earth’s attraction will cause it to rotate in a halo. The telescope requires a larger initial y-velocity to stay near the hub as it is ‘lower’ in altitude with respect to the Earth. If the hub starts to rotate in halo and the additional y-velocity given to the telescope is not quite sufficient, they will appear to separate. The fact that the gravity gradient model appears to move the satellites closer together suggests that relative y-velocity ( $\Delta\dot{y}_o$ ) is slightly overestimated. In Figure 3, the y and z relative motions predicted by the gravity gradient model approximate the STK relative motion well.

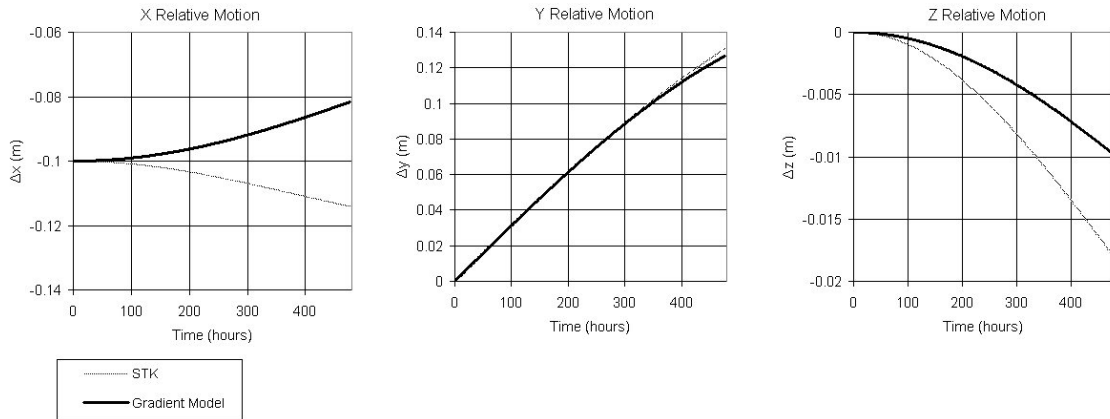


Figure 3: Model comparison of relative hub-telescope motion

The scenario introduced in Table 1 was implemented using the gravity gradient model and STK, and also compared to the Segerman and Zedd higher order model [13]. Similar relative motion results were achieved, although further investigation is required using alternative test cases, if available. A preliminary conclusion is that the higher order relative motion model will not necessarily offer significant improvement in formation modelling for controller design and that a linear (gravity gradient) model may be sufficient. The higher order model was also not found to provide improved values for initial conditions to optimise a halo formation in the numerical environment.

## Conclusion

A linearised gravity gradient model has been derived and evaluated for formation flying around L2. Initial model comparisons with STK scenarios have been performed and satisfactory model behaviour achieved. The Darwin scenario has demonstrated that the linearised model may be sufficiently accurate, particularly for continuous controller design.

Significant additional work is required involving the comparison of further test cases, and investigation of the sensitivity of the relative motion to initial conditions. Additions to the complexity of the linear model should be avoided until the magnitude of errors over a wider range of conditions has been established. Potential modelling improvements include extension of the model to the ER3BP, the inclusion of higher order terms, and the inclusion of Coriolis terms in the initial equations of motion. Eventually the model will be applied to controller design,

including sensor noise, and the formation-keeping and manoeuvring performance evaluated. Specific fuel balancing manoeuvring strategies will be investigated.

## References

- [1] ESA Concept and Feasibility Study Report, DARWIN The InfraRed Space Interferometer, *ESA-SCI(2000)12*, July 2000.
- [2] Farquhar, R.W., The Flight of the ISEE-3/ICE: Origins, Mission History, and a Legacy, 1998. Paper AIAA 98-4464.
- [3] Gurfil, P., Idan, M., Kasdin, N.J., Neurocontrol of Spacecraft Formation Flying in the Elliptic Restricted Three-Body Problem, *AIAA Guidance, Navigation and Control Conference and Exhibit*, 5-8 August 2002, Monterey, California, USA. Paper 2002-4962.
- [4] Gurfil, P., Kasdin, N.J., Dynamics and Control of Spacecraft Formation Flying in Three-Body Trajectories, *AIAA Guidance, Navigation and Control Conference*, 6-9 August 2001, Montreal, Canada. Paper AIAA 2001-4026.
- [5] Hamilton, N., Folta, D., Carpenter, R., Formation Flying Satellite Control around the L2 Sun-Earth Libration Point, *AIAA/AAS Astrodynamics Specialist Conference*, 5-8 August 2002, Monterey, California. Paper AIAA 2002-4528.
- [6] Hill, G.W., Researches in the Lunar Theory, *American Journal of Mathematics*, 1878.
- [7] Howell, K.C. Marchand, B.G., Control Strategies for Formation Flight in the Vicinity of the Libration Points, *AAS/AIAA Space Flight Mechanics Conference*, 9-13 February 2003, Ponce, Puerto Rico. Paper AAS 03-113.
- [8] Richardson, D.L., Analytic Construction of Periodic Orbits about the Collinear Points, *Celestial Mechanics* Vol.22, 1980.
- [9] Roberts, J.A., Roberts, P.C.E., 2004, The Development of High Fidelity J2 Models for Satellite Formation Flying Control, *AAS/AIAA Space Flight Mechanics Meeting*, February 8-12 2004, Maui, Hawaii. Paper AAS 04-162.
- [10] Schaub, H., Junkins, J.L., *Analytical Mechanics of Space Systems*, AIAA Education Series, Reston, USA, 2003.
- [11] Scheeres, D.J., Vinh, N.X., Dynamics and Control of Relative Motion in an Unstable Orbit, *AIAA/AAS Astrodynamics Specialist Conference*, 14-17 August 2000, Denver Colorado. Paper AIAA 2000-4135.
- [12] Schweighart, S., Sedwick, R., High-Fidelity Linearized J2 Model for Satellite Formation Flight, *Journal of Guidance, Control and Dynamics*, Vol.25 No.6, Nov-Dec 2002 pp1073-1080.
- [13] Segerman, A.M., Zedd, M.F., Preliminary Planar Formation-Flight Dynamics Near Sun-Earth L2 Point, *AAS/AIAA Space Flight Mechanics Meeting*, February 9-13 2003, Ponce, Puerto Rico. Paper AAS 03-133.
- [14] Vadali, S.R., Bae, H.-W., Alfriend, K.T., Design and Control of Libration Point Satellite Formations, *AAS/AIAA Space Flight Mechanics Conference*, Maui, Hawaii, 8-12 February 2004. Paper AAS 04-161.



# Development of a relative motion model for satellite formation flying around L2

Roberts, Jennifer A.

2004-12-18T10:57:38Z

---

<http://hdl.handle.net/1826/788>

*Downloaded from CERES Research Repository, Cranfield University*